mations are characterized by configurations with a high bond order and few occupied antibonding M-M MO's. Those $Mn_2(CO)_2$ configurations that favor a bridging carbonyl have common M-M MO's with $\sigma$, $\delta_{ip}$, $\sigma^*$, $\delta^*_{ip}$, and $\pi_{ip}$ character. Generally, when these $Mn_2(CO)_2$ configurations have more than one $a_g$ and more than two $b_u$ M-M MO's occupied, the extra $a_g$ and $b_u$ M-M MO's have $\pi^*_{ip}$ and $\sigma^*$ character, respectively. Thus, bent semibridging and symmetrically bridging conformations are characterized by configurations with a low bond order. The appearance of linear semibridging signifies strong metal-to-metal bonding.

In the previous work of Hall et al.[9a] and Benard et al.[1c] on linear semibridging carbonyls, linear semibridging was attributed to the maximization of the interaction between an occupied in-phase combination of metal d orbitals and one lobe of the carbonyl $2\pi$ orbital. Although orbital interactions like those previously described[9,10] exist here, they are not the primary origin of the observed structure. In many cases, these interactions may be a response to the linear semibridging structure forced upon the system by steric considerations. Thus, in this electronic interaction the system is attempting to minimize the repulsive interactions by creating an in-phase orbital combination.

In real compounds, as opposed to our simple $M_2(CO)_2$ model, it is much more difficult to resolve the competing effects of steric (repulsive) and bonding (attractive) interactions. The observed equilibrium geometry is, of course, a balance of both, and any distortions from this structure affect both interactions. In addition, both interactions are electronic in origin and cannot be separated in any rigorous way. Thus, the structure of a dimer is determined by inter- and intrafragment electronic effects (both steric and bonding) and one cannot predict from our model alone how a change in a non-bridging ligand or a change in the metal might modify the structure.

**Acknowledgment.** The authors wish to thank the National Science Foundation (Grant No. CHE 86-19420 and CHE 91-13634) and the Robert A. Welch Foundation (Grant No. A-648) for financial support, M. F. Guest for use of the program GAMESS, SERC Daresbury Laboratory, Warrington, WA4 4AD, U.K., and P. Sherwood and P. J. MacDougall for interactive MOPLOT. This research was conducted in part with the use of the Cornell National Supercomputer Facility, a resource for the Center for Theory and Simulation in Science and Engineering at Cornell University, which is funded in part by the National Science Foundation, New York State, and the IBM Corp., and in part at the Texas A&M University Supercomputer Center with a grant from Gray Research Inc.

**Registry No.** $Sc_2(CO)_2$, 138355-11-0; $Mn_2(CO)_2$, 54822-31-0.

# Solvent Effects. 3. Tautomeric Equilibria of Formamide and 2-Pyridone in the Gas Phase and Solution. An ab Initio SCRF Study

**Ming Wah Wong,[†] Kenneth B. Wiberg,*[,†] and Michael J. Frisch[‡]**

*Contribution from the Department of Chemistry, Yale University, New Haven, Connecticut 06511, and Lorentzian Inc., 127 Washington Avenue, North Haven, Connecticut 06473.*
*Received August 5, 1991*

**Abstract:** High level ab initio molecular orbital studies, using basis sets up to 6-31+G**, with electron correlation included at the second-order Møller-Plesset perturbation (MP2) and quadratic configuration interaction with singles and doubles (QCISD) levels, are reported for the tautomeric equilibria of formamide/formamidic acid and 2-pyridone/2-hydroxypyridine in the gas phase and solution. The solvent effects on the tautomeric equilibria were investigated by self-consistent reaction field (SCRF) theory. The calculated tautomerism free energy changes for 2-pyridone in the gas phase, cyclohexane, and acetonitrile are −0.64, 0.36, and 2.32 kcal mol$^{-1}$, in very good agreement with the experimental values (−0.81, 0.33, and 2.96 kcal mol$^{-1}$, respectively). The introduction of a dielectric medium has little effect on the electronic structure of the enol forms. On the other hand, significant effects on the molecular geometry, charge distributions, and vibrational frequencies are found for the more polar keto tautomers. The calculated changes are readily understood in terms of the increasing weight of the dipolar resonance structure.

## Introduction

The 2-pyridone/2-hydroxypyridine equilibrium represents one of the classic cases of medium-dependent tautomeric equilibrium.[1] In the gas phase, the preference of the hydroxy-form has been conclusively shown by IR, UV, mass spectrometric, and photoelectron experiments.[2] In nonpolar solvents such as cyclohexane, both tautomers exist in comparable amounts.[3] However, in solvents of high dielectric constant[3] and in the solid state,[4] the tautomeric equilibrium is shifted in favor of the more polar oxo-form. The dependence of such an equilibrium constant on solvent polarity has been reported previously by Frank and Katritzky[3a] and by Kuzuya et al.[3b] The theoretical prediction of the tautomerism energy of 2-pyridone has been the subject of intense interest in the past decade.[1d,5] Most ab initio calculations to date have focused on the relative stability of the two tautomeric forms

[†] Yale University.
[‡] Lorentzian Inc.

(1) (a) Katritzky, A. R.; Lagowski, J. M. *Adv. Heterocycl. Chem.* **1963**, *1*, 339. (b) Kwiatkowski, J. S.; Pullman, B. *Adv. Heterocycl. Chem.* **1975**, *18*, 199. (c) Pullman, B.; Pullman, B. *Adv. Heterocycl. Chem.* **1975**, *18*, 199. (d) Kwiatkowski, J. S.; Zielinski, T. J.; Rein, R. *Adv. Quantum Chem.* **1986**, *18*, 85.

(2) (a) Beak, P.; Fry, F. S. *J. Am. Chem. Soc.* **1973**, *95*, 1700. (b) Beak, P.; Fry, F. S., Jr.; Lee, J.; Steele, F. *J. Am. Chem. Soc.* **1976**, *98*, 171. (c) Beak, P. *Acc. Chem. Res.* **1977**, *10*, 186. (d) Nowak, M. J.; Sczepaniak, K.; Barski, A.; Shugar, D. *Z. Naturforsch.* **1978**, *33C*, 876. (e) Aue, D. H.; Betowski, L. D.; Davidson, W. R.; Bowers, M. T.; Beak, P.; Lee, J. *J. Am. Chem. Soc.* **1980**, *102*, 1174. (f) Brown, R. S.; Tse, A.; Vederas, J. C. *J. Am. Chem. Soc.* **1980**, *102*, 1174. (g) Nimlos, M. R.; Kelley, D. F.; Bernstein, E. R. *J. Phys. Chem.* **1989**, *93*, 643.

(3) (a) Frank, J.; Katritzky, A. R. *J. Chem. Soc., Perkin Trans. II* **1976**, 1428. (b) Kuzuya, M.; Noguchi, A.; Okuda, T. *J. Chem. Soc., Perkin Trans. II* **1985**, 1423.

0002-7863/92/1514-1645$03.00/0 

in the gas phase. Only, two studies[5c,6] have attempted to examine the tautomeric equilibrium in a polar medium.

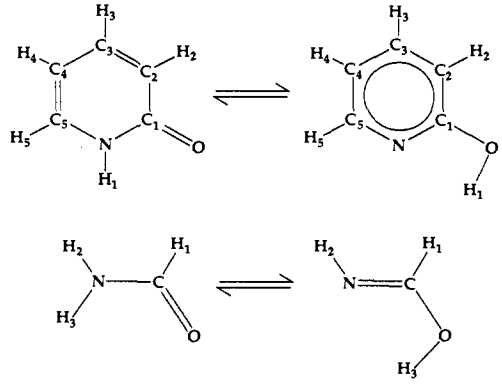

Recently, Onsager's reaction field model,[7] in the context of ab initio molecular orbital (MO) theory, has been shown to be a useful tool to study solvent–solute interaction.[8,9] Energy calculations including electron correlation using methods such as MP2 and QCISD[9] as well as analytical gradients[10] and second derivatives[10] for geometry optimizations and frequency calculations are now available. We have applied this solvation model to study several problems related to macroscopic (nonspecific) solvent effects and found that this method reproduced successfully the solvent effects on conformational equilibria and infrared absorption spectra.[9-12] In this paper, we use the ab initio reaction field theory to study the tautomeric equilibrium of 2-pyridone in a nonpolar solvent cyclohexane and in an aprotic polar solvent acetonitrile. We wished to see if the solvent effect on this equilibrium is reproduced by the reaction field theory. In addition, we have re-examined this keto–enol energy difference in the gas phase with various levels of theory with the aim to obtain a more definitive theoretical estimate.

We have also examined the tautomeric equilibrium of formamide, which represents the simplest model of keto–enol equilibrium. Knowledge of the energetics of tautomerism in these prototype systems in the gas and liquid phases may provide useful information on the intrinsic stability of other complex biologically important tautomers.

## Theoretical Methods and Results

Standard ab initio molecular orbital calculations[13] were performed using a development version of the Gaussian 91 series of programs.[14] Geometry optimizations for all structures were carried out with the 6-31G** basis set[13] at the Hartree–Fock (HF) level with $\epsilon = 1.0$ (corresponding to the gas phase), $\epsilon = 2.0$ (cyclohexane), and $\epsilon = 35.9$ (acetonitrile). Harmonic vibrational frequencies and infrared intensities were predicted at these equilibrium geometries. All molecules considered here were confirmed to be planar by the vibrational frequency calculations, which gave all real frequencies. The directly calculated zero-point vibrational energies (ZPEs) were scaled by 0.9 to account for the overestimation of vibrational frequencies at the HF level.[15] For the gas-phase structures, additional optimizations were performed at the HF/6-31G* and MP2/6-31G** levels. Improved relative energies were obtained through second-order Møller–Plesset (MP2)[16] and quadratic configuration interaction with singles and doubles (QCISD)[17] calculations with the larger 6-31+G** basis set based on the HF/6-31G** optimized geometries. The use of basis sets which include diffuse sp functions of heavy atoms has been shown to be particularly important for "solution" calculations of dipolar species.[9-11] To investigate further the effect of basis set and electron correlation on the tautomerism energies in the gas phase, we have also performed single-point energy calculations at the HF level with 6-31G*, 6-31G**, 6-31+G**, and 6-311G** basis sets,[13] and MP3 and MP4SDQ calculations[16] with the 6-31+G** basis set.

The effect of solute–solvent interaction was taken into account via the self-consistent reaction field (SCRF) method.[8f,9] This method is based on Onsager's reaction field theory[7] of electrostatic solvation. In the reaction field model, the solvent is considered as a uniform dielectric, characterized by a given dielectric constant $\epsilon$. The solute is assumed to occupy a spherical cavity of radius $a_0$ in the medium. The permanent dipole of the solute will induce a dipole (reaction field) in the surrounding medium, which in turn will interact with the molecular dipole to lead to stabilization. In the SCRF MO formalism, the solute–solvent interaction is treated as a perturbation of the Hamiltonian of the isolated molecule. The reaction field is updated iteratively until a self-consistency is achieved for the intramolecular electric field (cf. ref 9). The solvation energy calculated by the SCRF method corresponds to the electrostatic contribution to the free energy of solvation. In the present work, the cavity radii of the formamide/formamidic acid system ($a_0 = 3.15$ Å) and the 2-pyridone/2-hydroxypyridine system ($a_0 = 3.80$ Å) were calculated by a quantum mechanical approach.[12] This involves computing the 0.001 au electron density envelop (based on HF/6-31G** wave function) and scaling by 1.33 to obtain an estimate of molecular volume. To account for the nearest approach of solvent molecules 0.5 Å was added to the final $a_0$ value. In the case of formamide, this method has been shown to provide a better estimate of $a_0$ than the approach based on experimental molar volume.[10] Geometry optimizations and vibrational frequencies in the liquid phase were obtained using the recently developed analytical method of evaluating first and second derivatives of HF energy in the presence of a reaction field.[10] The cavity radius was fixed during these optimizations.

We have investigated the possibility of using an NMR spectroscopic method to study the tautomeric equilibrium of 2-pyridone in the gas phase. The chemical shifts of both oxo- and hydroxy-forms were calculated by the method of Kutzelnigg and Schindler (IGLO)[18] using the MP2/6-31G** optimized geome-

(4) (a) Wheeler, G. L.; Ammon, H. L. *Acta Crystallogr.* **1974**, *B30*, 680. (b) Almof, J.; Kvick, A.; Olovsson, I. *Acta Crystallogr.* **1971**, *B27*, 1201. (b) Penfold, B. *Acta Crystallogr.* **1953**, *6*, 591.

(5) (a) Moreno, M.; Miller, W. H. *Chem. Phys. Lett.* **1990**, *171*, 475. (b) Adamowicz, L. *Chem. Phys. Lett.* **1989**, *161*, 73. (c) Kwiatkowski, J. S.; Bartlett, R. J.; Person, W. B. *J. Am. Chem. Soc.* **1988**, *110*, 2353. (d) Cieplak, P.; Bash, P.; Chandra Singh, U.; Kollman, P. A. *J. Am. Chem. Soc.* **1987**, *109*, 6283. (e) Scanlan, M. J.; Hiller, I. H. *Chem. Phys. Lett.* **1984**, *107*, 330. (f) Scanlan, M. J.; Hiller, I. H.; McDowell, A. A. *J. Am. Chem. Soc.* **1983**, *105*, 3568. (g) Schlegel, H. B.; Gund, P.; Fluder, E. M. *J. Am. Chem. Soc.* **1982**, *104*, 5347.

(6) Karelson, M. M.; Katritzky, A. R.; Szafran, M.; Zerner, M. C. *J. Org. Chem.* **1989**, *54*, 6030.

(7) Onsager, L. *J. Am. Chem. Soc.* **1936**, *58*, 1486.

(8) (a) Mikkelson, K. V.; Agren, H.; Jensen, H. J. A.; Helgaker, T. *J. Chem. Phys.* **1988**, *89*, 3086. (b) Karelson, M. M.; Katritzky, A. R.; Zerner, M. C. *Int. J. Quantum Chem. Symp.* **1986**, *20*, 521. (c) Rivail, J. L.; Terryn, B.; Ruiz-Lopez, M. F. *J. Mol. Struct. (Theochem)* **1985**, *120*, 387. (d) Miertus, S.; Scrocco, E.; Tomasi, J. *Chem. Phys.* **1981**, *55*, 117. (e) Tapia, O. In *Molecular Interactions*; Orville-Thomas, W. J., Ed.; Wiley: New York, 1982; Vol. 3, Chapter 2. (f) Tapia, O.; Goscinski, O. *Mol. Phys.* **1975**, *29*, 1653.

(9) Wong, M. W.; Frisch, M. J.; Wiberg, K. B. *J. Am. Chem. Soc.* **1990**, *112*, 4776.

(10) Wong, M. W.; Wiberg, K. B.; Frisch, M. J. *J. Chem. Phys.*, In press.

(11) Wong, M. W.; Wiberg, K. B.; Frisch, M. J. *J. Am. Chem. Soc.*, In press.

(12) Wong, M. W.; Wiberg, K. B.; Frisch, M. J. *J. Am. Chem. Soc.* To be published.

(13) Hehre, W. J.; Radom, L.; Schleyer, P. v. R.; Pople, J. A. *Ab Initio Molecular Orbital Theory*; Wiley: New York, 1986.

(14) Frisch, M. J.; Head-Gordon, M.; Trucks, G. W.; Foresman, J. B.; Schlegel, H. B.; Raghavachari, K.; Robb, M. A.; Wong, M. W.; Replogle, E. S.; Binkley, J. S.; Gonzalez, C.; DeFrees, D. J.; Fox, D. J.; Whiteside, R. A.; Seeger, R.; Melius, C. F.; Baker, J.; Martin, R. L.; Kahn, L. R.; Stewart, J. J. P.; Topiol, S.; Pople, J. A. *GAUSSIAN 91* (Development Version, Revision B); Gaussian Inc.: Pittsburgh, PA, 1991.

(15) Pople, J. A.; Schlegel, H.; Raghavachari, K.; DeFrees, D. J.; Binkley, J. S.; Frisch, M. J.; Whiteside, R. F.; Hout, R. F.; Hehre, W. J. *Int. J. Quantum Chem. Symp.* **1981**, *15*, 269.

(16) (a) Møller, C.; Plesset, M. S. *Phys. Rev.* **1934**, *46*, 618. (b) Pople, J. A.; Binkley, J. S.; Seeger, R. *Int. J. Quantum Chem. Symp.* **1976**, *10*, 1.

(17) Pople, J. A.; Head-Gordon, M.; Raghavachari, K. *J. Chem. Phys.* **1987**, *87*, 5968.

(18) (a) Kutzelnigg, W. *Isr. J. Chem.* **1980**, *19*, 193. (b) Schindler, M.; Kutzelnigg, W. *J. Chem. Phys.* **1982**, *76*, 1919. (c) Kutzelnigg, W. *J. Mol. Struct.* **1989**, *202*, 11.

**Table I.** Optimized Geometries for Formamide and Formamidic Acid

| | gas phase | | | | solution[a,b] | |
|---|---|---|---|---|---|---|
| | HF/6-31G* | HF/6-31G** | MP2/6-31G** | expt[c] | $\epsilon = 2.0$ | $\epsilon = 35.9$ |
| | | | Formamide | | | |
| $r$(C–N) | 1.349 | 1.348 | 1.360 | 1.360 | −0.004 | −0.010 |
| $r$(C–O) | 1.193 | 1.193 | 1.223 | 1.219 | 0.003 | 0.008 |
| $r$(C–$H_1$) | 1.091 | 1.092 | 1.100 | 1.098 | 0.000 | −0.001 |
| $r$(N–$H_2$) | 0.996 | 0.994 | 1.005 | 1.002 | 0.000 | 0.000 |
| $r$(N–$H_3$) | 0.993 | 0.991 | 1.002 | 1.002 | 0.001 | 0.002 |
| ∠NCO | 124.95 | 124.89 | 124.79 | 124.5 | 0.19 | 0.54 |
| ∠$H_1$CO | 112.66 | 112.75 | 112.13 | 112.7 | −0.01 | −0.09 |
| ∠$H_2$CN | 119.33 | 119.14 | 118.82 | 118.8 | 0.19 | 0.62 |
| ∠$H_3$CN | 121.79 | 121.64 | 121.68 | 121.4 | −0.05 | −0.04 |
| | | | Formamidic Acid | | | |
| $r$(C–N) | 1.246 | 1.246 | 1.273 | | 0.000 | 0.000 |
| $r$(C–O) | 1.329 | 1.328 | 1.349 | | 0.000 | 0.001 |
| $r$(C–$H_1$) | 1.079 | 1.081 | 1.087 | | 0.000 | −0.001 |
| $r$(N–$H_2$) | 1.002 | 1.001 | 1.016 | | 0.000 | 0.000 |
| $r$(O–$H_3$) | 0.953 | 0.948 | 0.971 | | 0.000 | 0.000 |
| ∠OCN | 122.53 | 122.56 | 121.66 | | −0.13 | −0.28 |
| ∠$H_1$CN | 126.85 | 126.73 | 128.10 | | 0.06 | 0.14 |
| ∠$H_2$NC | 111.74 | 111.70 | 110.00 | | −0.07 | −0.09 |
| ∠$H_3$OC | 108.10 | 108.29 | 105.37 | | −0.11 | −0.35 |

[a] SCRF calculations ($a_0$ = 3.15 Å). [b] Change from the gas phase to solution (HF/6-31G**). [c] Taken from ref 21.

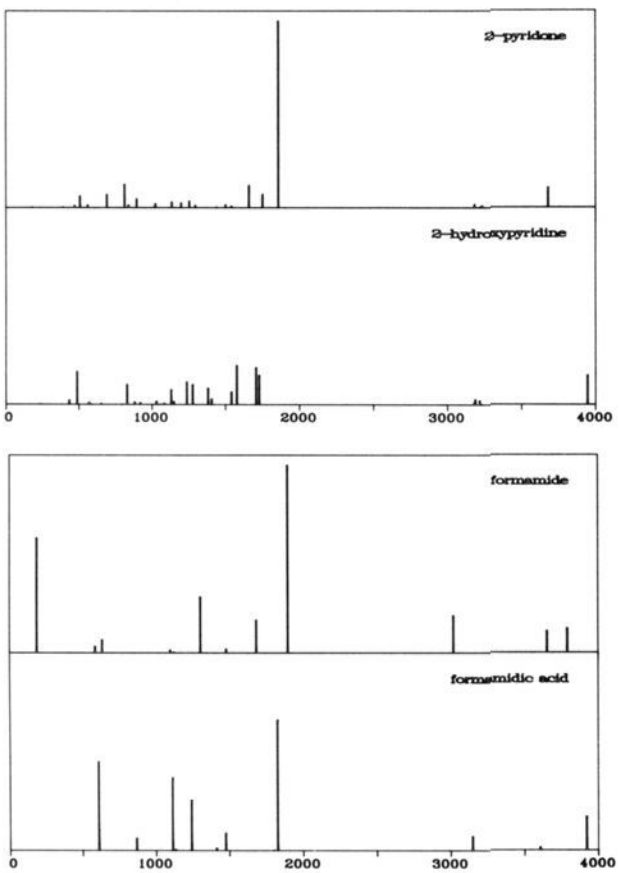


**Figure 1.** Computed IR spectra of 2-pyridone, 2-hydroxypyridine, formamide, and formamidic acid.

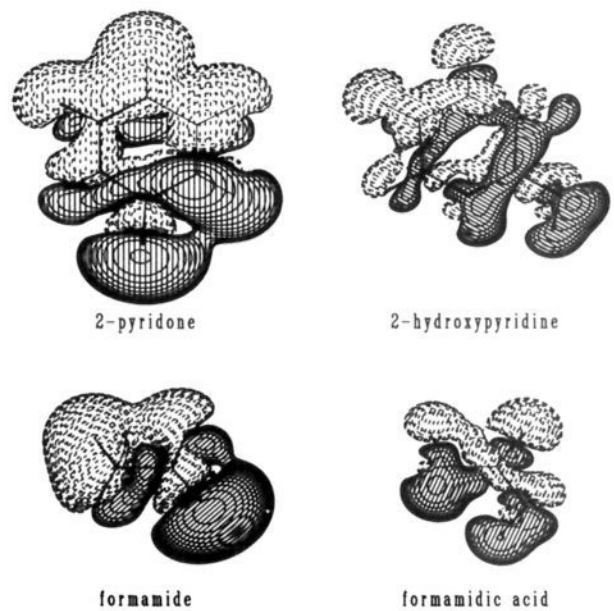


**Figure 2.** Charge density difference plots for 2-pyridone, 2-hydroxypyridine, formamide, and formamidic acid in going from the gas phase to a polar medium (using the same gas-phase geometry). The oxygen atom is shown to the right and the nitrogen atom to the left. The contour level is $1 \times 10^{-4}$ e/B$^3$. The full lines indicate electron density increases and dotted lines indicate decreases.

tries. The charge distributions in the gas phase and solution were examined using Bader's theory of atoms in molecules.[19] The electron populations were derived by numerical integration of the charge densities, using the boundary conditions derived by Bader's theory.[19] The charge densities were obtained from the HF/6-31+G** calculations based on the HF/6-31G** optimized geometries. In addition, we have calculated covalent bond orders based on a scheme proposed by Cioslowski and Mixon.[20] The analysis of the wave functions was carried out with PROAIM program.[21] The bond orders were calculated using BONDER.[20]

The results of the geometry optimizations are summarized in Tables I and II. The total energies and relative energies in the gas phase are given in Table III. Computed NMR chemical shifts for 2-pyridone and 2-hydroxypyridine are given in Table IV. Calculated entropies, enthalpies, zero-point energies, free energies, dipole moments, and thermal corrections are summarized in Tables V and VI. Vibrational frequencies and infrared intensities of

(19) (a) Bader, R. F. W. *Acc. Chem. Res.* **1985**, *9*, 18. (b) Bader, R. F. W. *Atoms in Molecules. A Quantum Theory*; Oxford University Press: New York, 1990.

(20) Cioslowski, J.; Mixon, S. T. *J. Am. Chem. Soc.* **1991**, *113*, 4142.
(21) Biegler-Konig, F. W.; Bader, R. F. W.; Tang, T.-H. *J. Comput. Chem.* **1982**, *3*, 317.

Table II. Optimized Geometries for 2-Pyridone and 2-Hydroxypyridine

| | gas phase | | | solid | solutions[a,b] | |
|---|---|---|---|---|---|---|
| | HF/6-31G* | HF/6-31G** | MP2/6-31G** | expt[c] | $\epsilon$ = 2.0 | $\epsilon$ = 35.9 |
| | | | 2-Pyridone | | | |
| $r(N-C_1)$ | 1.383 | 1.382 | 1.404 | 1.401 | −0.002 | −0.005 |
| $r(C_1-C_2)$ | 1.457 | 1.457 | 1.449 | 1.444 | −0.002 | −0.005 |
| $r(C_2-C_3)$ | 1.343 | 1.342 | 1.367 | 1.334 | 0.001 | 0.003 |
| $r(C_3-C_4)$ | 1.438 | 1.438 | 1.422 | 1.421 | −0.001 | −0.004 |
| $r(C_4-C_5)$ | 1.339 | 1.339 | 1.363 | 1.371 | 0.000 | 0.001 |
| $r(C_1-O)$ | 1.203 | 1.203 | 1.234 | 1.236 | 0.003 | 0.008 |
| $r(N-H_1)$ | 0.997 | 0.996 | 1.011 | | 0.000 | 0.000 |
| $r(C_2-H_2)$ | 1.073 | 1.073 | 1.080 | | 0.000 | 0.000 |
| $r(C_3-H_3)$ | 1.076 | 1.076 | 1.082 | | 0.000 | 0.000 |
| $r(C_4-H_4)$ | 1.072 | 1.072 | 1.078 | | 0.000 | 0.000 |
| $r(C_5-H_5)$ | 1.073 | 1.074 | 1.080 | | 0.000 | 0.000 |
| $\angle NC_1C_2$ | 113.65 | 113.69 | 112.55 | 112.7 | 0.02 | 0.02 |
| $\angle C_1C_2C_3$ | 121.15 | 121.12 | 122.05 | 122.3 | 0.01 | 0.02 |
| $\angle C_2C_3C_4$ | 121.51 | 121.51 | 121.22 | 122.2 | 0.01 | 0.06 |
| $\angle C_3C_4C_5$ | 117.59 | 117.59 | 118.13 | 116.0 | −0.04 | −0.12 |
| $\angle OC_1N$ | 120.51 | 120.49 | 120.38 | 121.3 | 0.02 | 0.05 |
| $\angle H_1NC_1$ | 114.78 | 114.75 | 113.74 | | 0.13 | 0.32 |
| $\angle H_2C_2C_1$ | 116.29 | 116.33 | 116.23 | | 0.05 | 0.18 |
| $\angle H_3C_3C_2$ | 119.66 | 119.62 | 119.41 | | 0.04 | 0.09 |
| $\angle H_4C_4C_3$ | 121.41 | 121.44 | 121.73 | | 0.04 | 0.10 |
| $\angle H_5C_5C_4$ | 123.37 | 123.27 | 123.80 | | −0.01 | 0.01 |
| | | | 2-Hydroxypyridine | | | |
| $r(N-C_1)$ | 1.307 | 1.308 | 1.331 | | 0.000 | 0.000 |
| $r(C_1-C_2)$ | 1.396 | 1.396 | 1.399 | | −0.001 | −0.001 |
| $r(C_2-C_3)$ | 1.373 | 1.372 | 1.386 | | 0.000 | 0.001 |
| $r(C_3-C_4)$ | 1.395 | 1.395 | 1.398 | | 0.000 | −0.001 |
| $r(C_4-C_5)$ | 1.374 | 1.374 | 1.388 | | 0.000 | 0.000 |
| $r(C_1-O)$ | 1.336 | 1.335 | 1.385 | | 0.001 | 0.003 |
| $r(O-H_1)$ | 0.951 | 0.946 | 0.969 | | 0.000 | 0.000 |
| $r(C_2-H_2)$ | 1.073 | 1.073 | 1.080 | | 0.000 | 0.000 |
| $r(C_3-H_3)$ | 1.075 | 1.076 | 1.081 | | 0.000 | 0.000 |
| $r(C_4-H_4)$ | 1.073 | 1.073 | 1.080 | | 0.000 | 0.000 |
| $r(C_5-H_5)$ | 1.075 | 1.076 | 1.083 | | 0.000 | 0.000 |
| $\angle NC_1C_2$ | 124.02 | 123.98 | 124.29 | | 0.04 | 0.12 |
| $\angle C_1C_2C_3$ | 117.22 | 117.24 | 117.58 | | −0.02 | −0.04 |
| $\angle C_2C_3C_4$ | 119.70 | 119.71 | 119.30 | | −0.01 | −0.02 |
| $\angle C_3C_4C_5$ | 117.53 | 117.53 | 118.32 | | 0.02 | 0.04 |
| $\angle OC_1N$ | 117.74 | 117.75 | 117.38 | | −0.09 | −0.26 |
| $\angle H_1OC_1$ | 107.93 | 108.12 | 105.13 | | −0.15 | −0.47 |
| $\angle H_2C_2C_1$ | 119.94 | 119.92 | 119.83 | | 0.03 | 0.10 |
| $\angle H_3C_3C_2$ | 119.97 | 119.95 | 120.12 | | 0.03 | 0.06 |
| $\angle H_4C_4C_3$ | 121.59 | 121.64 | 121.31 | | −0.04 | −0.07 |
| $\angle H_5C_5C_4$ | 120.73 | 120.67 | 120.98 | | −0.02 | −0.03 |

[a] SCRF calculations ($a_0$ = 3.80 Å). [b] Change from the gas phase to solution (HF/6-31G**). [c] Taken from ref 4c.

Table III. Calculated Total Energies (hartrees) and Relative Energies ($\Delta E$,[a] kcal mol$^{-1}$) in the Gas Phase

| level | formamide | formamidic acid | $\Delta E$ | 2-pyridone | 2-hydroxypyridine | $\Delta E$ |
|---|---|---|---|---|---|---|
| HF/6-31G*//HF/6-31G* | −168.930 70 | −168.908 01 | −14.24 | −321.567 25 | −321.567 11 | −0.09 |
| HF/6-31G**//HF/6-31G* | −168.940 48 | −168.920 23 | −12.70 | −321.578 36 | −321.580 81 | 1.54 |
| HF/6-31G**//HF/6-31G** | −168.940 49 | −168.920 25 | −12.70 | −321.578 37 | −321.580 84 | 1.55 |
| HF/6-31+G*//HF/6-31G** | −168.948 40 | −168.928 00 | −12.80 | −321.589 07 | −321.591 03 | 1.23 |
| HF/6-311G**//HF/6-31G** | −168.982 22 | −168.962 31 | −12.49 | −321.644 98 | −321.646 88 | 1.19 |
| MP2/6-31G**//MP2/6-31G** | −169.432 58 | −169.412 71 | −12.47 | −322.601 45 | −322.604 89 | 2.16 |
| HF/6-31+G**//MP2/6-31G** | −168.946 49 | −168.925 52 | −13.16 | −322.585 78 | −322.588 49 | 1.70 |
| MP2/6-31+G**//MP2/6-31G** | −169.448 61 | −169.428 39 | −12.69 | −322.620 79 | −322.625 20 | 2.77 |
| MP3/6-31+G**//MP2/6-31G**[b] | −169.443 20 | −169.426 27 | −10.62 | −322.609 89 | −322.613 55 | 2.30 |
| MP4SDQ/6-31+G**//MP2/6-31G**[b] | −169.453 72 | −169.434 68 | −11.95 | −322.623 33 | −322.623 35 | 0.01 |
| QCISD/6-31+G**//MP2/6-31G**[b] | −169.454 46 | −169.435 87 | −11.67 | −322.625 18 | −322.626 07 | 0.56 |

[a] $\Delta E$(enol−keto). [b] Frozen-core approximation.

all species are summarized in Tables VII and VIII, and the corresponding IR spectra are given in Figure 1. Finally, the calculated electron populations are given in Table IX, and the electron density difference plots in going from the gas phase to a polar medium ($\epsilon$ = 35.9) are given in Figure 2. Throughout this paper, bond lengths are given in angstroms and bond angles in degrees.

## Geometrical Structures

Previous theoretical studies[5a,b] suggested that perhaps the use of basis sets which include p-polarization functions on hydrogens is important for the structure of 2-pyridone and 2-hydroxypyridine. Here, we have carried out geometry optimizations for both tautomers at both HF/6-31G* and HF/6-31G** levels. As seen in Tables I and II, the optimized geometries are relatively unaffected by the inclusion of p-polarization functions on hydrogen atoms. Geometry optimizations with the inclusion of electron correlation (MP2/6-31G**) are reported for the first time for 2-pyridone and 2-hydroxypyridine. Significant effects appear to be associated with the incorporation of electron correlation. The changes are, however, systematic in that the calculated bond lengths at the MP2 level are uniformly longer than the corresponding Hartree–Fock

**Table IV.** Calculated NMR Chemical Shifts (ppm) for 2-Pyridone and 2-Hydroxypyridine[a]

| | 2-pyridone | | 2-hydroxy-pyridine | | |
|---|---|---|---|---|---|
| atom | $\sigma^b$ | $\delta^c$ | $\sigma^b$ | $\delta^c$ | diff |
| O | 21.3 | 260.4 | 177.3 | 104.4 | 156.0 |
| N | 74.7 | 173.7 | −54.1 | 302.5 | −128.8 |
| $C_1$ | −13.4 | 203.8 | 9.0 | 181.4 | 22.4 |
| $C_2$ | 72.9 | 117.5 | 65.3 | 125.1 | −7.6 |
| $C_3$ | 31.2 | 159.1 | 36.3 | 154.1 | 5.1 |
| $C_4$ | 84.9 | 105.5 | 56.4 | 134.0 | 28.5 |
| $C_5$ | 55.9 | 134.5 | 10.4 | 180.0 | −45.5 |
| $H_1$ | 21.1 | 10.1 | 28.8 | 2.4 | 7.7 |
| $H_2$ | 25.8 | 5.4 | 24.2 | 7.0 | −1.6 |
| $H_3$ | 23.9 | 7.3 | 23.2 | 8.0 | −0.7 |
| $H_4$ | 25.3 | 5.9 | 23.5 | 7.7 | −1.8 |
| $H_5$ | 24.4 | 6.8 | 21.8 | 9.4 | −2.6 |

[a] HF/DZP calculations based on MP2/6-31G** geometries. [b] Values relative to the bare nucleus. [c] Values relative to methane for carbons and hydrogens, water for oxygens, and ammonia for nitrogens.

values. Geometry optimizations at the MP2 level generally provide good agreement with experimental data,[13] as can be seen in the comparison of the structure of formamide with that from the gas-phase experiment[22] in Table I. For 2-pyridone, several bond lengths and bond angles are known in the solid state.[4c] The structural parameters calculated at the MP2/6-31G** level are also in good agreement with the experiment values (Table II). Thus, we expect that the MP2 optimized geometries of 2-hydroxypyridine will be reliable.

The calculated changes in structure in going from the gas phase to solutions are given in Tables I and II. As one might have expected, the introduction of a solvent reaction field has little effect on the calculated geometry of formamidic acid and 2-hydroxypyridine. In contrast, significant changes in molecular geometry are predicted for the more polar keto tautomers. The calculated C–N and C–O bond lengths of formamide and 2-pyridone are found to be altered by 0.005–0.010 Å in going from the gas phase to a solvent of dielectric constant 35.9. These changes, lengthening of C–O bonds and shortening of C–N bonds, correspond to a small increase in the weight of the dipolar resonance structure. The importance of the dipolar resonance structure in solution is further supported by the calculation of *covalent* bond orders. For instance, the C–O bond order decreases from 1.13 to 1.08 and the C–N bond order increases from 0.89 to 0.94 in going from the gas phase to a polar medium.

**Tautomeric Energies**

The relative stability of 2-pyridone and 2-hydroxypyridine in the gas phase has been the subject of numerous ab initio studies.[1d,5] A large variation of the tautomerism energy, −3.5 to +2.1 kcal mol$^{-1}$, has been reported using various levels of ab initio theory.[5] Here, we attempt to establish a more definitive theoretical estimate of the relative energy by considering the effect of basis set and electron correlation in greater detail. The calculated tautomerization energy of 2-pyridone in the gas phase using various theoretical levels of theory is summarized in Table III. Consistent with previous findings,[5a,b] inclusion of p-polarization functions on hydrogen has a significant effect on the relative energy (by 1.6 kcal mol$^{-1}$). On the other hand, the effects of including diffuse sp functions on heavy atoms and expanding the basis set from double-$\zeta$ to triple-$\zeta$ are small. As mentioned in the previous section, p-polarization functions on hydrogen have a small effect on the molecular geometry. Therefore, the use of 6-31G* and 6-31G** geometries gives essentially the same results. The same trends of basis set effects are found with the tautomerism energy of formamide (Table III). Different levels of electron correlation, using the 6-31+G** basis set, are found to have different effects on the tautomerization energy of 2-pyridone. MP2 and MP3 levels increase the relative energy, whereas higher treatments of electron correlation at MP4SDQ and QCISD levels reduce the relative energy. At the QCISD/6-31G**//MP2/6-31G** level, 2-hydroxypyridine is more stable than 2-pyridone by 0.6 kcal mol$^{-1}$. Zero-point energy (ZPE) corrections at the HF/6-31G** level favor the hydroxy-form by 0.2 kcal mol$^{-}$ (Table VI), in good accord with the experimental estimate by Beak (0.1 kcal mol$^{-1}$).[2c] However, this calculated $\Delta$ZPE value is considerably less than those reported previously (0.7–1.2 kcal mol$^{-1}$).[5] Thus, our final best estimate of the tautomerism energy of 2-pyridone is 0.8 kcal mol$^{-1}$, in good agreement with the experimental value (0.3 kcal mol$^{-1}$).[2b] For formamide, our best estimate of tautomerization energy at the QCISD/6-31+G**//MP2/6-31G** + ZPE level is 12.5 kcal mol$^{-1}$, in close agreement with the experimental estimate, 11 ± 4 kcal mol$^{-1}$.[5f]

Although the tautomeric equilibrium of 2-pyridone in the gas phase has been studied by various spectroscopic techniques, no NMR spectroscopic study has yet been reported. To investigate the possibility of using this experimental technique to study the tautomeric equilibrium, we have calculated the chemical shifts of 2-pyridone and 2-hydroxypyridine using the IGLO method.[18] The calculations were based on the MP2/6-31G** optimized geometries and the results are summarized in Table IV. The observed proton NMR shifts in DMSO (10.1, 6.4, 7.5, 6.2, and 7.4 ppm for $H_1$, $H_2$, $H_3$, $H_4$, and $H_5$, respectively)[23] are well reproduced by the calculated values of 2-pyridone (10.1, 5.4, 7.3, 5.9, and 6.8, respectively). Large differences in chemical shifts are predicted for O, N, $C_1$, $C_4$, and $H_5$ of the 2-pyridone/2-hydroxypyridine system. Thus, the NMR spectrum (e.g. $^{13}$C of $C_1$) at low temperatures should be well resolved and clearly indicate the presence of the two tautomers, and it should be possible to determine the equilibrium constant from the change in chemical shifts with temperature.

As seen in Tables V and VI, the calculated dipole moments (at the MP2/6-31+G** level) of the keto tautomers are larger than the corresponding enol forms, by almost 3 D. Thus, one would expect a differential solvent stabilization in solution. For instance, in a nonpolar solvent of $\epsilon$ = 2.0, 2-pyridone is computed to have larger stabilization energy (1.2 kcal mol$^{-1}$) than 2-hydroxypyridine (0.2 kcal mol$^{-1}$). This differential solvent stabilization effect is even more pronounced in a polar medium of $\epsilon$ = 35.9. Thus, a reversal of stability is predicted for the 2-pyridone/2-hydroxypyridine system in a polar medium. These results are consistent with experimental observations of 2-pyridone is condensed phases.[3,4] As with 2-pyridone, formamide is preferentially stabilized in solution. One important observation that comes from the $\Delta E$ calculations of the formamide/formamidic acid system at different levels of theory is that the difference between QCISD and MP2 values is almost unchanged in going from the gas phase to solutions. The QCISD-MP2 corrections of $\Delta E$ for formamide are 0.86, 0.87, and 0.88 kcal mol$^{-1}$, for $\epsilon$ = 1.0, 2.0, and 35.9, respectively. Similar results have also been obtained for the energy difference between the keto and enol forms of acetaldehyde.[24] Thus, for the 2-pyridone/2-hydroxypyridine system, we have employed the QCISD-MP2 correction in the gas phase to estimate the "solution" $\Delta E$ values at the QCISD level. The tautomeric equilibrium constants of 2-pyridone in solvents of different polarity have been determined by UV spectroscopic experiments, and −log $K_T$ values of 0.24 and 2.17 were measured for the tautomeric equilibrium in cyclohexane and acetonitrile.[3a] These values correspond to free energies ($\Delta G$) of 0.33 and 2.96 kcal mol$^{-1}$, respectively, calculated from the expression $\Delta G = -RT \ln K$. As with gas-phase free energy, the prediction of $\Delta G$ in solution requires correctsion for internal energy and entropy.[10] A correction term for solute concentration is required to calculate the total entropy in solution. However, this term should be essentially the same for two tautomers and has negligible effect in the highly dilute solution in which this equilibrium was observed. The details of the computation of $\Delta G$ in the gas and liquid phases are sum-

(22) Brown, R. D.; Godfrey, P. D.; Kleibomer, B. J. *J. Mol. Struct.* **1987**, *124*, 34.

(23) *Nuclear Magnetic Resonance Spectra. The Standard Sadlter Spectra*; Sadtler Research Laboratories: Philadelphia, 1990.

(24) Wong, M. W.; Wiberg, K. B.; Frisch, M. J. Unpublished results.

**Table V.** Calculated Energies[a,b] and Dipole Moments ($\mu$) of Formamide and Formamidic Acid in the Gas Phase and Solutions (Cyclohexane and Acetonitrile)

| | formamide | | | formamidic acid | | |
|---|---|---|---|---|---|---|
| | $\epsilon = 1.0$ | $\epsilon = 2.0$ | $\epsilon = 35.9$ | $\epsilon = 1.0$ | $\epsilon = 2.0$ | $\epsilon = 35.9$ |
| | | | Absolute Value | | | |
| $E$(HF/6-31G**) | −168.980 49 | −168.943 10 | −168.947 35 | −168.920 25 | −168.920 47 | −168.920 81 |
| $E$(HF/6-31+G**) | −168.948 40 | −168.951 30 | −168.956 13 | −168.928 00 | −168.928 27 | −168.928 70 |
| $E$(MP2/6-31+G**) | −169.446 17 | −169.448 83 | −169.453 32 | −169.426 01 | −169.426 25 | −169.426 65 |
| $E$(QCISD/6-31+G**) | −169.463 86 | −169.466 51 | −169.471 01 | −169.445 07 | −169.445 31 | −169.445 73 |
| ZPE | 30.79 | 30.89 | 31.00 | 31.55 | 31.52 | 31.47 |
| $H - H_0$ | 2.34 | 2.27 | 2.20 | 2.02 | 2.02 | 2.03 |
| $S$[c] | 61.52 | 60.97 | 60.48 | 59.51 | 59.53 | 59.57 |
| $\mu$[d] | 3.90 | 4.20 | 4.72 | 1.18 | 1.24 | 1.34 |
| | | | Relative Value | | | |
| $\Delta E$(HF/6-31G**) | 12.70 | 14.20 | 16.65 | | | |
| $\Delta E$(HF/6-31+G**) | 12.80 | 14.45 | 17.21 | | | |
| $\Delta E$(MP2/6-31+G**) | 12.65 | 14.17 | 16.74 | | | |
| $\Delta E$(QCISD/6-31+G**) | 11.79 | 13.30 | 15.86 | | | |
| $\Delta$(ZPE)[e] | 0.69 | 0.573 | 0.42 | | | |
| $\Delta E$[f] + $\Delta$(ZPE)[e] | 12.48 | 13.87 | 16.28 | | | |
| $\Delta(H - H_0)$ | −0.32 | −0.25 | −0.17 | | | |
| $\Delta H$[f] | 12.16 | 13.62 | 16.11 | | | |
| $-T\Delta S$ | 0.60 | 0.43 | 0.27 | | | |
| $\Delta G$[f] | 12.76 | 14.05 | 16.38 | | | |

[a] Based on HF/6-31G** geometries; at room temperature (298 K). [b] $E$ in hartrees; ZPE, $H - H_0$, $\Delta E$, $\Delta H$, $-T\Delta S$, and $\Delta G$ in kcal mol$^{-1}$; and $S$ in cal mol$^{-1}$ K$^{-1}$. [c] The solution entropies were calculated using the gas phase translational partition coefficient. The change in $S$ on going from the gas phase to solution should be essentially the same for the tautomers. The solute concentration term was not included. [d] MP2/6-31+G** values; in D. [e] Scaled by 0.9. [f] Based on $\Delta E$ calculated at the QCISD/6-31+G** level.

**Table VI.** Calculated Energies[a,b] and Dipole Moments ($\mu$) of 2-Pyridone and 2-Hydroxypyridine in the Gas Phase and Solutions (Cyclohexane and Acetonitrile)

| | 2-pyridone | | | 2-hydroxypyridine | | |
|---|---|---|---|---|---|---|
| | $\epsilon = 1.0$ | $\epsilon = 2.0$ | $\epsilon = 35.9$ | $\epsilon = 1.0$ | $\epsilon = 2.0$ | $\epsilon = 35.9$ |
| | | | Absolute Value | | | |
| $E$(HF/6-31G**) | −321.578 37 | −321.580 30 | −321.583 73 | −321.580 84 | −321.581 03 | −321.581 36 |
| $E$(HF/6-31+G**) | −321.589 07 | −321.591 22 | −321.595 14 | −321.591 03 | −321.591 25 | −321.591 64 |
| $E$(MP2/6-31+G**) | −322.620 79 | −322.622 68 | −322.626 34 | −322.625 20 | −322.625 45 | −322.625 90 |
| ZPE | 63.32 | 63.33 | 63.33 | 63.13 | 63.11 | 63.08 |
| $H - H_0$ | 3.10 | 3.09 | 3.08 | 3.06 | 3.06 | 3.06 |
| $S$[c] | 72.83 | 72.78 | 72.69 | 72.38 | 72.39 | 72.42 |
| $\mu$[d] | 4.20 | 4.68 | 5.57 | 1.46 | 1.61 | 1.90 |
| | | | Relative Value | | | |
| $\Delta E$(HF/6-31G**) | −1.55 | −0.46 | 1.49 | | | |
| $\Delta E$(HF/6-31+G**) | −1.23 | −0.02 | 2.20 | | | |
| $\Delta E$(MP2/6-31+G**) | −2.77 | −1.74 | 0.28 | | | |
| $\Delta E$(QCISD/6-31+G**)[e] | −0.56 | 0.47 | 2.49 | | | |
| $\Delta$(ZPE)[f] | −0.17 | −0.20 | −0.23 | | | |
| $\Delta E$[g] + $\Delta$(ZPE)[f] | −0.73 | 0.27 | 2.26 | | | |
| $\Delta(H - H_0)$ | −0.04 | −0.03 | −0.02 | | | |
| $\Delta H$[g] | −0.77 | 0.24 | 2.24 | | | |
| $-T\Delta S$ | 0.13 | 0.12 | 0.08 | | | |
| $\Delta G$[g] | −0.64 | 0.36 | 2.32 | | | |

[a] Based on HF/6-31G** geometries; at room temperature (298 K). [b] $E$ in hartrees; ZPE, $H - H_0$, $\Delta E$, $\Delta H$, $-T\Delta S$, and $\Delta G$ in kcal mol$^{-1}$; and $S$ in cal mol$^{-1}$ K$^{-1}$. [c] The solution entropies were calculated using the gas phase translational partition coefficient. The change in $S$ on going from the gas phase to solution should be essentially the same for the tautomers. The solute concentration term was not included. [d] MP2/6-31+G** values. [e] QCISD − MP2 corrections (2.21 kcal mol$^{-1}$) were estimated from the gas-phase calculations (see text). [f] Scaled by 0.9. [g] Based on $\Delta E$ calculated at the QCISD/6-31+G** level.

marized in Tables V and VI. The enthalpy of the tautomerization reaction, $\Delta H$, was obtained by adding the zero-point energy correction, $\Delta$(ZPE), and the thermal correction, $\Delta(H - H_0)$ to $\Delta E$, and the final $\Delta G$ value was computed from the equation $\Delta G = \Delta H - T\Delta S$, where $\Delta S$ is the entropy change. Our theoretical estimates of tautomerization free energy for 2-pyridone with $\epsilon$ = 1.0, 2.0, and 35.9 are −0.64, 0.36, and 2.32 kcal mol$^{-1}$, in very good agreement with the experimental estimates (−0.81, 0.33, and 2.96 kcal mol$^{-1}$, respectively).[2b,3a] Thus, the dependence of the tautomeric equilibrium of 2-pyridone on solvent polarity is well-reproduced by the ab initio SCRF calculations. These results provide another example of the usefulness of the reaction field theory in providing both qualitative and quantitative understanding of the solvent effects on chemical equilibrium.

Finally, it is important to note that the solvation free energy calculated at the QCISD level is also satisfactorily reproduced by HF and MP2 calculations. For instance, the calculated solvation free energies for formamide in acetonitrile solution ($\epsilon$ = 35.9) are 4.85 and 4.49 kcal mol$^{-1}$ for HF and MP2 levels, respectively, and compare well to our best estimate of 4.49 kcal mol$^{-1}$ at the QCISD level. However, a more accurate treatment of electron correlation (QCISD) is important for the computation of absolute free energy in solution.

### Vibrational Frequencies and Infrared Spectra

The gas-phase infrared spectra of 2-pyridone and 2-hydroxypyridine have been examined recently by Moreno and Miller using a similar level of theory (HF/DZP(d,p)).[5a] As suggested by these authors, the N—H ($\nu_1$) and C=O ($\nu_6$) stretching frequencies of 2-pyridone as well as the O–H ($\nu_1$) stretching frequency of 2-hydroxypyridine can be used to differentiate between the two tautomeric forms. This is clearly shown in the computed spectra

**Table VII.** Calculated Vibrational Frequencies[a] ($cm^{-1}$) and Infrared Intensities (km $mol^{-1}$) of Formamide and Formamidic Acid[b]

| | | formamide | | | | | | | formamidic acid | | | | | |
|---|---|---|---|---|---|---|---|---|---|---|---|---|---|---|
| | | frequency | | | | intensity | | | frequency | | | intensity | | |
| | | $\epsilon = 1$ | | | | | | | | | | | | |
| | | calc | expt[e] | $\epsilon = 2$[c] | $\epsilon = 36$[c] | $\epsilon = 1$ | $\epsilon = 2$[d] | $\epsilon = 36$[d] | $\epsilon = 1$ | $\epsilon = 2$[c] | $\epsilon = 36$[c] | $\epsilon = 1$ | $\epsilon = 2$[d] | $\epsilon = 36$[d] |
| A′ | $\nu_1$ | 3632 | 3545 | −6 | −16 | 65 | 15 | 39 | 3775 | 1 | 4 | 91 | 3 | 6 |
| | $\nu_2$ | 3500 | 3451 | −4 | −10 | 58 | 13 | 44 | 3454 | 0 | −2 | 8 | 1 | 5 |
| | $\nu_3$ | 2893 | 2852 | 4 | 11 | 101 | 4 | 8 | 3015 | 3 | 8 | 38 | 0 | −1 |
| | $\nu_4$ | 1758 | 1734 | −16 | −43 | 510 | 68 | 186 | 1692 | −5 | −14 | 355 | 3 | 85 |
| | $\nu_5$ | 1560 | 1572 | 2 | 4 | 89 | 9 | 24 | 1366 | −1 | −2 | 47 | 5 | 13 |
| | $\nu_6$ | 1370 | 1378 | 1 | 1 | 11 | 5 | 18 | 1308 | −1 | −1 | 6 | 1 | 1 |
| | $\nu_7$ | 1208 | 1255 | 5 | 13 | 152 | 12 | 32 | 1151 | −2 | −6 | 137 | 7 | 15 |
| | $\nu_8$ | 1016 | 1030 | 5 | 10 | 8 | −2 | −5 | 1032 | −3 | −10 | 198 | 31 | 89 |
| | $\nu_9$ | 543 | 565 | 1 | 2 | 17 | 3 | 9 | 565 | −2 | −5 | 57 | 8 | 20 |
| A″ | $\nu_{10}$ | 1040 | 1059 | 4 | 8 | 2 | 0 | 0 | 1049 | 1 | 1 | 3 | 0 | 0 |
| | $\nu_{11}$ | 588 | 602 | 7 | 16 | 35 | −4 | −11 | 803 | 1 | 2 | 33 | 0 | 0 |
| | $\nu_{12}$ | 174 | 289 | 59 | 136 | 312 | 18 | 44 | 565 | −10 | −25 | 241 | 10 | 24 |

[a] Scaled by 0.91 if over 2000 $cm^{-1}$ and 0.88 if under 2000 $cm^{-1}$. [b] Calculated at the HF/6-31G** level. [c] Frequency shift from the gas phase to solution. [d] Intensity change from the gas phase to solution. [e] Taken from ref 25.

**Table VIII.** Calculated Vibrational Frequencies[a] ($cm^{-1}$) and Infrared Intensities (km $mol^{-1}$) of 2-Pyridone and 2-Hydroxypyridine[b]

| | | 2-pyridone | | | | | | 2-hydroxypyridine | | | | | |
|---|---|---|---|---|---|---|---|---|---|---|---|---|---|
| | | frequency | | | intensity | | | frequency | | | intensity | | |
| | | $\epsilon = 1$ | $\epsilon = 2$[c] | $\epsilon = 36$[c] | $\epsilon = 1$ | $\epsilon = 2$[d] | $\epsilon = 36$[d] | $\epsilon = 1$ | $\epsilon = 2$[c] | $\epsilon = 36$[c] | $\epsilon = 1$ | $\epsilon = 2$[d] | $\epsilon = 36$[d] |
| A′ | $\nu_1$ | 3525 | 0 | 2 | 88 | 11 | 30 | 3780 | 0 | 1 | 130 | 16 | 40 |
| | $\nu_2$ | 3099 | 3 | 7 | 8 | −2 | −6 | 3092 | −1 | −1 | 2 | 0 | 1 |
| | $\nu_3$ | 3091 | −1 | −4 | 5 | 2 | 1 | 3082 | 0 | 2 | 19 | 1 | 3 |
| | $\nu_4$ | 3078 | 4 | 8 | 2 | −1 | 9 | 3054 | 1 | 3 | 24 | 0 | 0 |
| | $\nu_5$ | 3050 | 1 | 3 | 14 | 1 | 1 | 3048 | 1 | 2 | 10 | 4 | 10 |
| | $\nu_6$ | 1721 | −15 | −41 | 830 | 164 | 449 | 1600 | 0 | −1 | 131 | 11 | 30 |
| | $\nu_7$ | 1622 | −2 | −8 | 60 | 16 | 80 | 1581 | −1 | −2 | 164 | 24 | 64 |
| | $\nu_8$ | 1537 | −2 | −6 | 99 | 21 | 64 | 1461 | −2 | −5 | 174 | 22 | 56 |
| | $\nu_9$ | 1427 | −2 | −5 | 7 | 0 | 1 | 1427 | −1 | −2 | 56 | 15 | 48 |
| | $\nu_{10}$ | 1390 | 0 | 0 | 13 | 2 | 9 | 1302 | 1 | 1 | 24 | 3 | 9 |
| | $\nu_{11}$ | 1333 | −1 | −3 | 3 | 2 | 10 | 1280 | −2 | −6 | 73 | 14 | 41 |
| | $\nu_{12}$ | 1200 | 0 | −1 | 9 | −1 | −3 | 1183 | −1 | −2 | 88 | 14 | 36 |
| | $\nu_{13}$ | 1163 | 0 | 1 | 29 | 6 | 18 | 1147 | −1 | −2 | 100 | 24 | 72 |
| | $\nu_{14}$ | 1111 | 1 | 3 | 21 | 5 | 18 | 1064 | −1 | −2 | 12 | 1 | 1 |
| | $\nu_{15}$ | 1052 | 0 | −1 | 25 | 4 | 12 | 1048 | 0 | −1 | 65 | 17 | 52 |
| | $\nu_{16}$ | 949 | 0 | −1 | 17 | 4 | 8 | 1003 | 0 | 1 | 4 | 1 | 3 |
| | $\nu_{17}$ | 941 | 2 | 5 | 4 | 1 | 7 | 954 | 0 | 1 | 14 | 2 | 6 |
| | $\nu_{18}$ | 778 | 2 | 5 | 12 | 0 | 0 | 817 | −1 | −2 | 10 | 3 | 9 |
| | $\nu_{19}$ | 583 | 1 | 3 | 0 | 0 | 0 | 605 | 0 | 0 | 3 | 1 | 3 |
| | $\nu_{20}$ | 519 | 0 | 0 | 11 | 3 | 11 | 538 | 0 | 0 | 1 | 0 | 0 |
| | $\nu_{21}$ | 436 | 0 | 0 | 9 | 2 | 5 | 402 | 0 | −2 | 19 | 3 | 10 |
| A″ | $\nu_{22}$ | 998 | 1 | 4 | 0 | 0 | 0 | 990 | 1 | 3 | 0 | 0 | 0 |
| | $\nu_{23}$ | 952 | 4 | 11 | 0 | 0 | 0 | 973 | 1 | 2 | 0 | 0 | 0 |
| | $\nu_{24}$ | 830 | −1 | −2 | 38 | −3 | −9 | 852 | 1 | 2 | 7 | −1 | −2 |
| | $\nu_{25}$ | 753 | 3 | 8 | 103 | 8 | 20 | 769 | 0 | −1 | 88 | 4 | 10 |
| | $\nu_{26}$ | 714 | 2 | 6 | 1 | −1 | −1 | 734 | 0 | 0 | 0 | 0 | 0 |
| | $\nu_{27}$ | 641 | 2 | 4 | 58 | 7 | 17 | 527 | 0 | −1 | 8 | 0 | −1 |
| | $\nu_{28}$ | 470 | 1 | 2 | 51 | 3 | 7 | 452 | −5 | −14 | 145 | 8 | 20 |
| | $\nu_{29}$ | 363 | 1 | 4 | 3 | −1 | −1 | 407 | 0 | 0 | 0 | 1 | 2 |
| | $\nu_{30}$ | 168 | 3 | 9 | 2 | 0 | 0 | 217 | 0 | 0 | 1 | 0 | 1 |

[a] Scaled by 0.91 if over 2000 $cm^{-1}$ and 0.88 if under 2000 $cm^{-1}$. [b] Calculated at the HF/6-31G** level. [c] Frequency shift from the gas phase to solution. [d] Intensity change from the gas phase to solution.

in Figure 1. Relatively large infrared intensities are predicted for these absorption bands for experimental estimate of the oxo/hydroxy concentration ratio. For formamide, the gas-phase spectrum has been studied previously.[25] Our scaled calculated spectrum is in good agreement with the observed spectrum (root-mean-square error = 38 $cm^{-1}$).

As with other carbonyl compounds, large frequency shifts upon solvation are calculated for the carbonyl stretching vibrations of formamide and 2-pyridone. In both cases, a red shift of about 40 $cm^{-1}$ is predicted in going from the vapor phase to acetonitrile solution. These results are in good accord with the large carbonyl frequency shifts observed for formamide[10] and *N*-methyl-2-pyridone.[26] For the case of formamide, significant frequency shifts are also calculated for $\nu_1$, $\nu_7$, and $\nu_{12}$ vibrational modes. In particular, a sizable shift of 136 $cm^{-1}$ is predicted for the lowest vibrational mode ($\nu_{12}$). Smaller changes in vibrational frequencies in going from vacuo to solution are computed for the less polar enol compounds, formamidic acid and 2-hydroxypyridine. The infrared intensities of most absorption bands are calculated to become more intense in going from the gas phase to cyclohexane to acetonitrile.

### Charge Distributions

The charge distributions of dipolar compounds are often altered significantly in the presence of a solvent reaction field.[9-11] We have examined the charge distributions of all tautomers in both the gas phase and in a polar medium using Bader's theory of atoms

(25) (a) Evans, J. C. *J. Chem. Phys.* **1954**, *22*, 1228. (b) King, S. T. *J. Phys. Chem.* **1971**, *75*, 405.

(26) Bellamy, J. L.; Rogash, P. E. *Spectrochim. Acta* **1960**, *16*, 30.

Table IX. Calculated Electron Populations[a]

| | formamide | | | formamidic acid | | |
|---|---|---|---|---|---|---|
| atom | $\epsilon = 1.0$ | $\epsilon = 35.9$ | Δ | $\epsilon = 1.0$ | $\epsilon = 35.9$ | Δ |
| C | 4.037 | 4.040 | 0.003 | 4.214 | 4.217 | 0.003 |
| N | 8.490 | 8.494 | 0.004 | 8.525 | 8.528 | 0.003 |
| O | 9.395 | 9.406 | 0.011 | 9.334 | 9.332 | −0.002 |
| $H_1$ | 1.023 | 1.019 | −0.004 | 0.988 | 0.982 | −0.006 |
| $H_2$ | 0.520 | 0.519 | −0.001 | 0.601 | 0.599 | −0.002 |
| $H_3$ | 0.535 | 0.523 | −0.012 | 0.340 | 0.342 | 0.002 |
| total | 24.000 | 24.001 | | 24.002 | 24.000 | |
| | 2-pyridone | | | 2-hydroxypyridine | | |
| atom | $\epsilon = 1.0$ | $\epsilon = 35.9$ | Δ | $\epsilon = 1.0$ | $\epsilon = 35.9$ | Δ |
| $C_1$ | 4.237 | 4.258 | 0.021 | 4.558 | 4.575 | 0.017 |
| $C_2$ | 5.950 | 5.959 | 0.009 | 5.911 | 5.910 | −0.001 |
| $C_3$ | 5.974 | 5.968 | −0.006 | 5.963 | 5.961 | −0.002 |
| $C_4$ | 5.871 | 5.851 | −0.020 | 5.952 | 5.947 | −0.005 |
| $C_5$ | 5.433 | 5.450 | 0.017 | 5.233 | 5.239 | 0.006 |
| N | 8.600 | 8.601 | 0.001 | 8.654 | 8.658 | 0.004 |
| O | 9.414 | 9.437 | 0.023 | 9.335 | 9.334 | −0.001 |
| $H_1$ | 0.514 | 0.518 | 0.004 | 0.339 | 0.343 | 0.004 |
| $H_2$ | 0.992 | 1.017 | 0.025 | 1.001 | 1.003 | 0.002 |
| $H_3$ | 1.012 | 0.999 | −0.013 | 1.016 | 1.007 | −0.009 |
| $H_4$ | 1.017 | 0.982 | −0.035 | 1.027 | 1.016 | −0.011 |
| $H_5$ | 0.990 | 0.966 | −0.024 | 1.013 | 1.011 | −0.002 |
| total | 50.004 | 50.006 | | 50.002 | 50.004 | |

[a] HF/6-31+G**//HF/6-31G** wavefunctions.

in molecules.[19] As expected, the charge distributions of formamide enol and 2-hydroxypyridine are found to be slightly influenced by a dielectric medium. However, a larger degree of charge separation is predicted for the more polar keto compounds, formamide and 2-pyridone. This difference in reaction field effect on charge distributions is in accord with the changes in dipole moments, molecular geometry, and vibrational frequencies in going from the gas-phase to solution. However, the charge distribution in solution is more delocalized than one would have expected from the dipolar resonance picture. For the keto compounds, the electron populations at the carbonyl oxygens increase in going from vacuo to a polar volume medium, by 0.11 and 0.23 e for formamide and 2-pyridone, respectively (Table IX). Consistent with previous observations for other carbonyl compounds,[27] the change in charge at oxygen does not come from the carbon, but instead comes from the hydrogens. In fact, an increase in electron population is predicted for the carbonyl carbon. It is interesting to note that the electron populations of $C_4$ and $C_5$ of 2-pyridone are also perturbed by the reaction field. The changes in electron density in the presence of a solvent reaction field for formamide and 2-pyridone are shown pictorially in Figure 2. It can be seen that the electron density is transferred from the hydrogens to the carbonyl moiety, which leads to a larger degree of charge separation. The SCRF wave functions were obtained using the unrelaxed (gas-phase) geometries in order to make a direct comparison of the effects of solvation.

## Conclusions

Several important points emerge from this study:

(1) Geometry optimizations at the correlated level (MP2/6-31G**) are reported for the first time for 2-hydroxypyridine and 2-pyridone. NMR spectroscopy is predicted to offer another means of studying the tautomerization of 2-pyridone in the gas phase.

(2) The solvent effects on the tautomeric equilibrium of 2-pyridone are readily reproduced by ab initio reaction field theory. The calculated tautomerism free energies in the gas phase, cyclohexane, and acetonitrile are in very good agreement with the experimental estimates.

(3) High-level treatment of electron correlation, such as QCISD, is essential for a reliable estimate of the tautomerism energy of 2-pyridone in both the gas phase and solution. However, SCRF calculations at the HF and MP2 levels can provide reasonable estimates of solvation free energy.

(4) The calculated changes in geometry, charge distributions, and infrared spectra of the keto tautomers in going from the gas phase to solution are in accord with the increasing weight of the dipolar resonance structure.

**Acknowledgment.** This research was supported by a grant from the National Institutes of Health and by Lorentzian, Inc.

**Registry No.** 2-Pyridone, 142-08-5; 2-pyridinol, 72762-00-6; formamide, 75-12-7; formimidic acid, 60100-09-6.

(27) Wiberg, K. B.; Wong, M. W. To be published.

# Group Electronegativities from the Bond Critical Point Model

**Russell J. Boyd*,† and Susan L. Boyd‡**

*Contribution from the Departments of Chemistry, Dalhousie University, Halifax, Nova Scotia, Canada B3H 4J3, and Mount Saint Vincent University, Halifax, Nova Scotia, Canada B3M 2J6.*
*Received August 19, 1991*

**Abstract:** The bond critical point model is used to calculate the electronegativities of over 100 groups from ab initio wave functions. The data show that the electronegativity of a group is largely determined by the connecting atom: atoms that are one bond or more removed have very little effect on the electronegativity of a group. The small effect of atoms one bond or more removed, however, is consistent with qualitative predictions: the higher the electronegativity of B for a given A, the greater the electronegativity of group −AB. Two other trends of note are, firstly, that increasing unsaturation in the vicinal bond increases electronegativity and, secondly, that protonation increases electronegativity of a group while deprotonation decreases it.

Few chemical concepts are as enduring and as widely used as that of electronegativity, "the power of an atom in a molecule to attract electrons to itself".[1] The popularity of the concept is due to its simplicity and to the availability of numerical values for most of the elements. In general, numerical scales indicate that electronegativity increases from left to right within a given row of the periodic table and decreases from top to bottom. Numerous correlations between atomic electronegativities and a variety of

† Dalhousie University.
‡ Mount Saint Vincent University.

(1) Pauling, L. *The Nature of the Chemical Bond*, 3rd ed.; Cornell University: Ithaca, NY, 1960, and references therein.

0002-7863/92/1514-1652$03.00/0 